is followed by the D-domain which is further divided into two structurally distinct sub-segments, the shoulder (D_S) and the arm (D_a) segments. These sub-segments are stabilized by a number of disulfide bonds and bound calcium ions (see Section 2.3.). The D_S-segment protrudes from the M-domain, and is opposed to the catalytic site and close to calcium-binding site I. This calcium-binding site is highly conserved among canonical ADAMs [24,31]. The D-domain, together with the C-domain, forms C-shaped arm with its concave surface toward the M-domain. Notably, the distal portion of the C-domain comes close to and faces toward the catalytic site in the M-domain. The residues that are important for stabilizing the MDC domain architecture (e.g. the number and spacing of cysteinyl residues and the residues that coordinate the calcium ions) are strictly conserved in the primary structures of all known ADAMs, with the exception of the atypical ADAMs (ADAM10 and 17, see Section 2.3.) [24,31]. The canonical membrane-bound ADAMs contain an EGF domain following the C-domain, however, no roles have been assigned to this domain. The EGF domain probably works as a rigid spacer connecting the MDC domain with and orienting it against the membrane-spanning region.

2.1. Metalloproteinase (M) domain

The structures of the M-domains of mammalian ADAM/ADAMTS family proteins determined to date can be superimposed, with variability only in the peripheral loop regions [28,29,32–34]. They can also be superimposed on SVMPs of different sub-classes [24–26,35]. The M-domain has an oblate ellipsoidal shape with a notch in its flat side that creates a relatively small "lower" domain and an "upper" main domain in the "standard" orientation [12] (Fig. 2B). The catalytic zinc ion is situated at the bottom of the cleft, and is tetrahedrally coordinated by the Nε2 atoms of the three histidines in the consensus sequence HEXXHXXGXXHD (Fig. 2C). The glutamic acid functions as a catalytic base that polarizes a water molecule involved in nucleophilic attack at the sessile peptide bond. The side-chain of the conserved methionine (called Met-turn) downstream of the catalytic consensus sequence provides a hydrophobic base beneath the three zinc-coordinating histidine side-chains. All of these structural features are hallmarks of the metzincin clan of metalloendopeptidases [12,13]. The upper domain has a central core consisting of a highly twisted five-stranded β-sheet and four α-helices, while the C-terminal lower domain consists of a helix and an irregularly folded region (Fig. 2B). This irregularly folded region is important for substrate recognition because it forms, in part, the wall of the S1' crevice. Fig. 2C depicts a close-up view of the active site cleft of catrocollastatin/VAP2B in complex with a hydroxamic inhibitor GM6001 [25]. The peptidic portion of the inhibitor adopts an extended geometry and binds to the notched right-hand side of the active-site cleft of the M-domain, mimicking the C-terminal part of enzyme-bound substrate from left to right. The inhibitor forms hydrogen bonds with the adjacent strand and the loop region, in essence extending the central β-sheet by two strands. The mode of peptidic inhibitor binding to catrocollastatin/VAP2B is essentially the same as that of its mammalian counterparts [28,29,32–34]. Although the M-domain catalytic site should recognize the sequence flanking the substrate cleavage site, ADAMs cleave broader assemblies of sites in membrane-anchored substrates, which indicates that there are no strict peptide bond requirements for cleavage [36]. Rather, the accessibility and structure of the cleavage site (juxtamembrane region), the distance from the membrane, and interactions distal to the cleavage site (exosite) that are mediated by non-catalytic ancillary domains are believed to be important determinants, either alone or in combination, for recognition and processing by membrane-bound ADAMs. Therefore, knowledge of the three-dimensional structure of the entire extracellular domain is necessary in order to fully understand the molecular mechanism of target recognition by ADAMs.

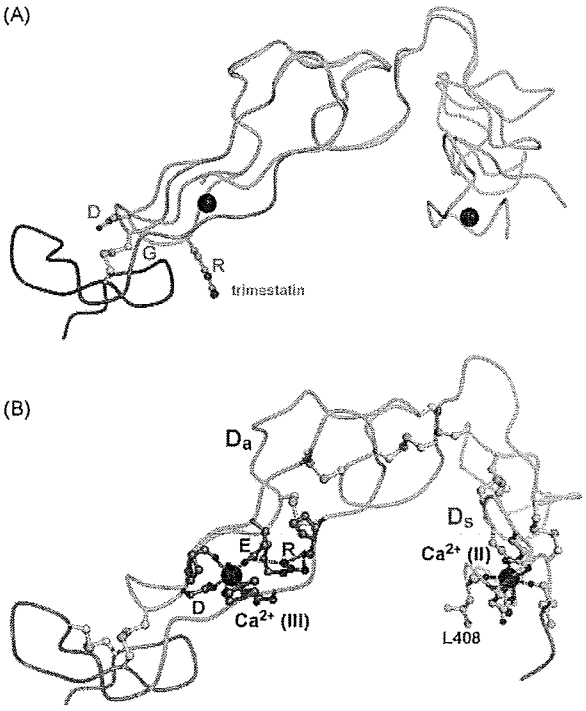

Fig. 3. D-domain structure. (A) Superimposition of the D_a-segments of catrocollastatin/VAP2B and trimestatin [41] (shown in light green). The Arg-Gly-Asp side chains in trimestatin and the disulfide bond between the D_a and C_w segments in catrocollastatin/VAP2B are shown in ball-and-stick representation. The D_s, D_a and C_h domains of catrocollastatin/VAP2B are in cyan, pink and gray, respectively. (B) Calcium-coordinating residues and disulfide bonds in the D-domain of catrocollastatin/VAP2B, which are strictly conserved in the canonical ADAMs [24,25]. The charged residues (R, D and E) in the putative integrin-binding sequence, RX_6DLPEF, and the pivotal L408 in the D_s/M joint are indicated.

2.2. Disintegrin-loop

The term "disintegrin" was initially used to describe a family of cysteine-rich, RGD-containing small (49–84 amino acids) proteins from viper venom that inhibited platelet aggregation and integrin-mediated cell-adhesion [37]. ADAMs are unique among non-venomous proteins in having a disintegrin-like sequence. The ability of venom disintegrins to bind integrins has been attributed to an extended loop (disintegrin-loop) containing a cell-adhesion sequence (e.g. RGD) [38]. Thus, the analogous region within the D-domain of ADAMs, which usually possesses EDC sequence instead of RGD, with the exception of human ADAM15, has been putatively assigned integrin binding function [16]. In support of this hypothesis, it has been widely reported that the disintegrin-loops of ADAMs interact with certain integrins (mostly non-αI-domain integrins), thereby mediating cell–cell and cell–matrix interactions [1,39]. The RGD-type integrin ligands are proposed to bind to non-αI-domain integrins by fitting into the crevice formed between the propeller and βA domains of the headpiece of the integrin [40]. The structures of SVMPs revealed that the D-domains of ADAMs have a similar structure as the RGD-containing disintegrin trimestatin [41], however, the disintegrin-loop is unavailable for protein-protein interactions due to steric hindrance [24–27,31] (Fig. 3A), which highlights a discrepancy in the hypothesis. The RX_6DLPEF sequence that encompasses the disintegrin-loop is suggested to be a candidate for integrin-binding [42], however, the crystal structure

data suggest that all three charged residues in this sequence (R, D and E) act primarily as structural elements, and are not expected to provide a protein-binding interface (Fig. 3B). Although a number of studies have shown a direct interaction between ADAMs and integrins, the precise function of the ADAM disintegrin-loop is still controversial, and further studies are needed to elucidate whether and how the interactions with integrins observed in model systems relates to the physiological functions of ADAMs.

2.3. Disintegrin-like (D) domain

The D-domain is linked to the M-domain by a short linker that allows variability in the orientation of the M-domain and the D_S-segment [24,31]. A conserved hydrophobic residue (L408 in catrocollastain/VAP2B) in the D_S segment, which points toward a small hydrophobic pocket in the M-domain, functions as the pivotal point [25]. The D_S and D_a segments consist largely of a series of turns and two short regions of antiparallel β-sheet, and constitute a continuous C-shaped arm structure, together with the N-terminal region of the C-domain, which is designated as the "wrist" (C_W) segment. The C_W-segment consists of a pair of antiparalel β-sheets and loops and packs against the D_a-segment on one side and against the C-terminal region of the "hand" (C_h) segment on the other. There are three disulfide bonds in the D_S-segment, three in the D_a-segment and one in the C_W-segment, and the segments are connected by single disulfide bonds (Fig. 3B). Both the D_S and the D_a segments contain structural calcium-binding sites, sites II and III, respectively, in which the conserved side-chain and the main-chain carboxyl oxygen atoms are involved in pentagonal bipyramidal coordination [24,25,31]. Because there are few secondary structural elements, bound calcium ions and the disulfide bonds are essential for the structural rigidity of the C-shaped arm structure of ADAMs.

ADAM10 and ADAM17 are atypical members of the mammalian ADAM family, as they lack calcium-binding sites I and III. Rather, ADAM10 and 17 have additional disulfide bonds in the M-domain and a shorter C_h-segment compared to the canonical ADAMs. They also lack the EGF domain. The Crystal structure of the DC-domain of bovine ADAM10 revealed a continuous D_a/C_W structure, however, the D_S-segment was partially disordered and the bound calcium ion was not identified in the D_S-segment [27], although calcium-binding is expected based on primary sequence.

2.4. Cysteine-rich "Hand" (C_h) domain and hyper-variable-region (HVR)

The core of the C-terminal region of the C-domain, the C_h-segment, has an α/β fold structure that consists of the two antiparallel β-strands packed against two of the three α-helices, and five disulfide bonds [24]. The C_h-segment of VAP1 has a novel fold with no structural homology to currently known proteins, except for the corresponding segments of other SVMPs [25,26], ADAM10 [27] and ADAMTSs (see Section 2.5.) [28,29]. The C_h-domain is characterized by a core region that is stabilized by conserved disulfide bridges, and peripheral variable loops that protrude from the core, providing extended surface areas that are most likely involved in protein-binding.

The loop that encompasses residues 562–582 and extends across the central region of the C_h-segment of VAP1 (blue regions in Fig. 2A, B and Fig. 4A, B, D) is the region in which the ADAM sequences are most divergent and variable in length (11–55 amino acid) (Fig. 4F). Therefore, this region has been designated as the hyper-variable region (HVR) [24]. The structures of the HVRs that have been determined to date are all in the crystal packing [24,25,27] or in the interface of the subunits [26], and show a relatively small number of direct interactions with the remaining core region, which suggests that they are flexible in solution. Because of its location within the molecule, opposed to the catalytic site, the HVR has been putatively assigned protein-binding functions [24] (see Section 4).

A helix-loop-helix segment found in VAP1 (residues 526–555), designated as the variable segment (shown in green color in Fig. 4C and boxed in green in Fig. 4F) is missing in the structures of ADAM10 [27] and ADAMTSs [28,29] (see below), replaced by a short loop. The residues in the variable segment seem to be rather mobile in solution because they have higher temperature factors [24,25,29] or are disordered in the crystal structures [27,28]. The variable segment is also characteristic of each ADAM and is located adjacent to the HVR. Thus, it might create an auxiliary protein-binding interface.

2.5. D-domain of ADAMTSs

The ADAMTS family is a branch of the ADAM family. Members of the ADAMTS family share a modular structure with the ADAMs, but have varying numbers of C-terminal thrombospondin type-1 (TSP1) repeats instead of a transmembrane segment. Thus, they constitute primarily secreted proteinases (Fig. 1). There are 19 ADAMTS proteins in humans, and they have been shown to function as aggrecanases, procollagen N-proteinases and von Willebrand factor (vWF) cleaving proteases [15]. Crystallographic studies on the MD fragments of ADAMTS-1, -4 and -5 revealed that the D-domains of ADAMTSs showed no structural homology to the D-domains of ADAMs, but were very similar in structure to the C_h-segments of ADAMs and other related proteins [28,29]. Despite low sequence identity, the topology and the location of the four disulfide bonds in the C_h-segments are conserved among these proteins (Fig. 4F). Thus, while the "disintegrin-like" nomenclature was used for ADAMTS family proteins due to sequence similarity [14], structural studies suggest that ADAMTS family proteins contain a C_h-domain, rather than a D-domain, immediately following the M-domain. Thus, the term D-domain for ADAMTS proteins appears to be a misnomer [28].

ADAMTSs lack $D_S/D_a/C_W$ segments, and the C_h-segment (previously referred to as the D-domain) is connected to the M-domain by a connector loop (22 residues in ADAMTS-1) that wraps around the back of the M-domain, resulting in a drastically different position of the C_h-segment relative to the M-domain as compared to VAP1 (Fig. 4A, B, D, and F). The structures of ADAMTS-4 and 5 [29] can be superimposed onto that of ADAMTS-1 [28] with slight differences in the relative orientations between the M-domain and the C_h-segment. Interestingly, the C_h-segments of ADAMTSs are located in close proximity to the active site and form, in part, the S3' pocket, thus potentially providing an auxiliary substrate-binding surface (Fig. 4E). Of note, the segment corresponding to the HVR in VAP1 runs across the middle of the C_h-segment of the ADAMTSs (Fig. 4E). In this configuration, the region downstream of the P3' residues of the substrate can bind directly to the HVR (Fig. 4E). In agreement with this, deletion of the P4'–P18' residues of vWF has been shown to abolish cleavage by recombinant MD-domain-containing ADAMTS13 [43]. Similar to the HVRs of ADAMs, the HVR segments of ADAMTSs are variable among the 20 human ADAMTSs, which suggests that the HVR in the ADAMTS proteins also provides an auxiliary substrate-binding site. The structures of the ADAMTS proteins support the idea that the HVR creates a protein-protein interaction interface in the C_h-segment, which is the newly identified adhesion module.

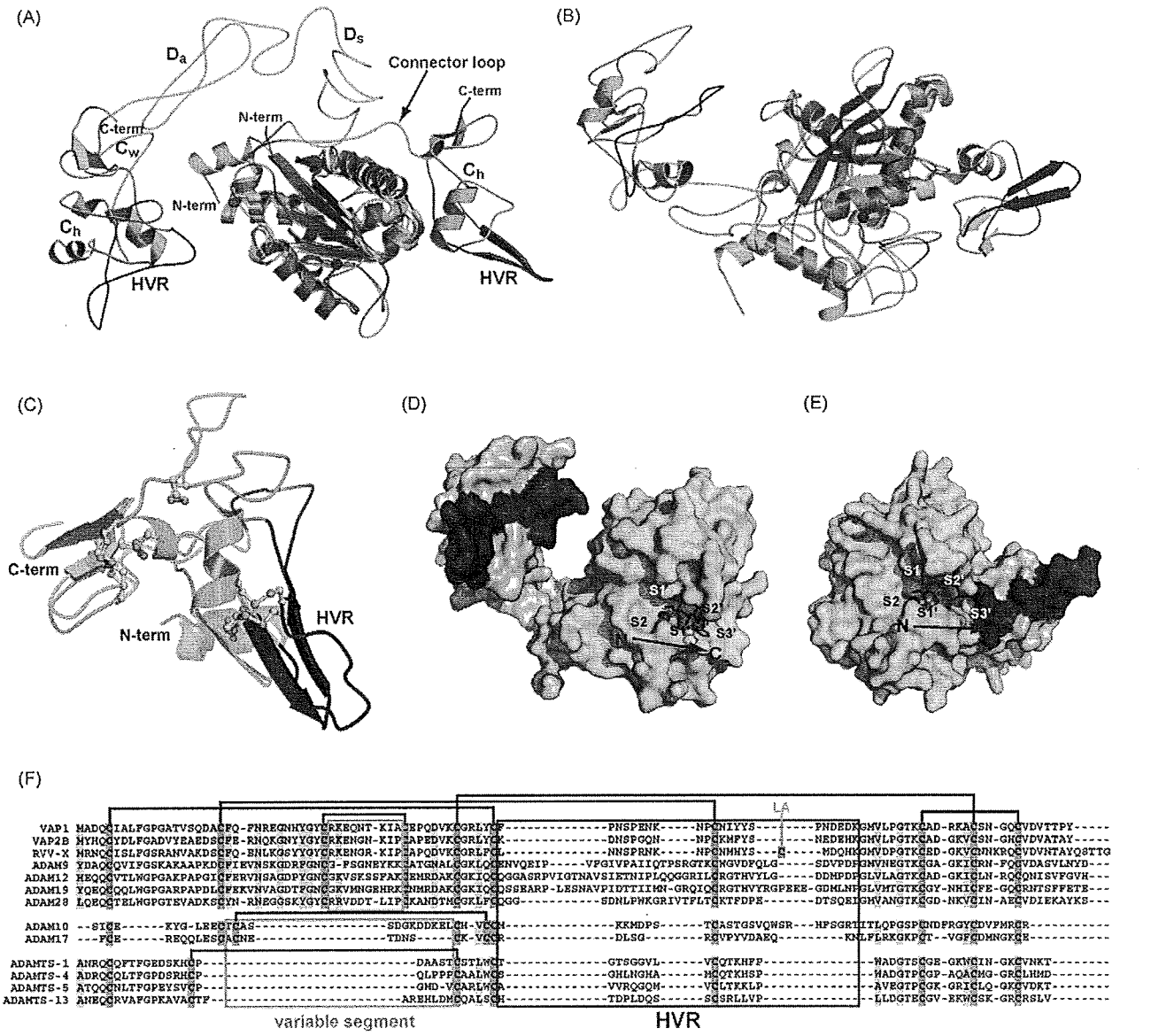

Fig. 4. Comparison of the structures of ADAMs and ADAMTSs. (A and B) Two orthogonal views of the superimposition of the M-domains of VAP1 (2ERP, shown in cyan) and ADAMTS-5 (2RJQ, shown in pink). The C_h-segments and the HVRs of each protein are shown in light green and blue, respectively. (C) Superimposition of the C_h-segment of VAP1 (shown in cyan, green and blue) and ADAMTS-5 (shown in pink, green and red). Surface representations of the VAP1 monomer (D) and ADAMTS-5 (E). The M-domains, C_h-segments, HVRs and bound peptidic inhibitors are shown in yellow, light green, blue and magenta, respectively. (F) Structure-based sequence alignment of SVMPs, human ADAMs and human ADAMTSs. The disulfide bonds are schematically indicated.

3. Adhesive functions of ADAMs

The D and C domains of ADAMs and related proteins have been suggested to be involved in protein-protein interactions. ADAM12 interacts with cell-surface syndecan through its C-domain and mediates integrin-dependent cell spreading [20]. The DC-domain of ADAM13 has been implicated in cell migration [44], and binds to the ECM proteins laminin and fibronectin [19]. ADAM13 C-domain was also found to be a major determinant for specific developmental events that are mediated by the proteolytic activity of ADAM13 [23]. Shedding of interleukin-1 receptor-II by ADAM17 requires the DC-domain [22]. Jararhagin-C and catrocollastatin-C, which are the DC domain-containing fragments of the P-III SVMPs jararhagin and catrocollastain/VAP2B, respectively, inhibit collagen-induced platelet aggregation [45,46]. The C-domain of atrolysin-A, another P-III SVMP, specifically binds collagen type I and vWF, and blocks collagen-vWF interactions [47,48] through binding to the vWF A-domain (VWA) [49]. It also binds to the VWA-containing ECM proteins collagen XII and XIV, and matrilins 1, 3 and 4 [50]. Two peptide sequences that are located on the surface of the C-domain of jararhagin have been shown to bind to vWF and block C-domain-binding to vWF [51], while another peptide that encompasses the HVR has been shown to interfere with the interaction between platelets and collagen [52]. It should be noted, however, that short peptides do not always mimic their counterparts in the folded protein, and most of the studies described above have not identified the specific regions of the C-domain that are involved. Thus, additional studies, including site directed mutagenesis based on crystal structures, will facilitate a better understanding of the adhesive mechanisms of ADAM family pro-

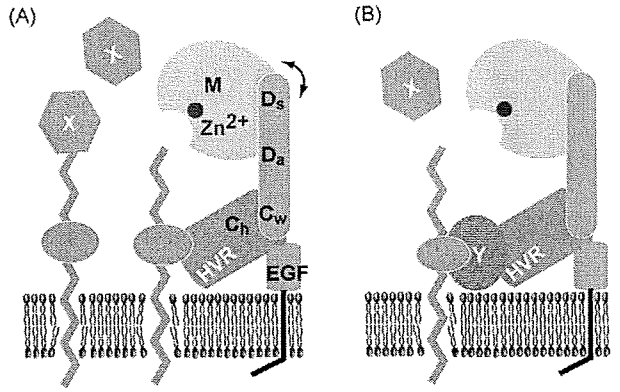

Fig. 5. Proposed models for shedding by ADAM family proteins. The membrane-bound ADAM molecule and a membrane-bound substrate molecule X are schematically drawn. (A) The substrate X is directly recognized by the HVR. (B) Substrate X is recognized by the HVR through an associated protein Y.

teins, and the interplay between their proteolytic and adhesive functions.

4. Roles of DC domains in shedding by ADAMs

In the VAP1 structure, the HVR segment is present at the distal end of the C-shaped MDC-domain, and points toward the catalytic site of the M-domain. ADAMs have distinct HVR sequences, which results in distinct molecular surface features that could be involved in determining the specificity of binding counterparts. This raises the intriguing possibility that the HVR creates an exosite for binding substrate molecules [24] (Fig. 5). The D-domain is opposed to and apart from the M-domain catalytic site. Thus, it may function primarily as a scaffold that spatially coordinates two functional sites (the catalytic site and the exosite). Flexibility between the sub-segments may be important for fine-tuning substrate recognition and allow slight adjustments to the spatial alignment of the catalytic site and exosite during the catalytic cycle [25].

Although the model in which the HVR captures substrates directly (Fig. 5A), or via binding to an associated protein (Fig. 5B), is still hypothetical, the crystal structure of RVV-X and the substrate-docking model shed some light on this issue [26]. RVV-X is a member of the P-IV class of SVMPs, which consists of an MDC-containing heavy chain and two C-type lectin-like light chains (CLPs) [30,53] (Fig. 1). The RVV-X crystal structure revealed that the CLP portion of RVV-X forms a putative exosite for binding to substrate (coagulation factor X) on the one hand, and directly interacts with the HVR in the heavy chain on the other, consistent with the model in Fig. 5B. The RVV-X crystal structure is a good illustration of evolutionary gain of specify of ADAMs, through HVR-mediated binding to other proteins to create an exosite for binding ligands.

The DC domain structure of ADAM10 revealed an acidic surface pocket, formed by the three glutamic acid residues in the C_h-segment, that could serve as a binding site for the ephrin/Eph complex when ADAM10 cleaves ephrin-A2 *in trans* [27]. These three residues are not within the HVR, however, they face the catalytic site in the M-domain when the D_a-segment of ADAM10 is superimposed with that of VAP1, because ADAM10 and VAP1 have different orientations between the C_w and C_h-segments [24]. The extensive molecular surface of the elongated DC domain arm of ADAMs could also provide protein-protein interaction sites, in addition to the HVR. The presence of multiple ligand-binding sites may help explain how the same ADAM can recognize multiple targets.

5. Conclusion

Increasing evidences for a role of ADAMs as sheddases in important biological processes and in numerous disease conditions is rapidly accumulating. However, fundamental aspects of ADAM function such as how ADAMs select their substrates and how activity is regulated, remain to be elucidated. Crystallographic studies shed new light on the structures and functions of ADAM family proteins, revealing potentially novel protein-protein interaction sites, and providing intriguing data for the development of working hypotheses. Individual ADAMs shed a wide array of substrates that do not share common features for recognition by ADAMs. Therefore, a model in which the HVR directs substrate specificity by binding directly to substrates is not likely to be a general mechanism. Additional structural and biochemical studies of ADAM-substrate interactions are necessary to elucidate the molecular mechanism of target recognition, identify the key substrates of ADAMs during specific biological events, and in importantly, to enable the design of selective inhibitors of this class of enzymes.

Acknowledgements

This work was supported in part by Grant-in-aid for Scientific Research B-19370047 from the Ministry of Education, Science, Sports and Culture, and Health and Labour Sciences Research Grants.

References

[1] White JM, Bidges L, DeSimone DW, Tomczuk M, Wolfsberg TG. Introduction to the ADAM family. In: Hooper NM, Lendeckel U, editors. The ADAM Family of Proteinases. Dordrecht, The Netherlands: Springer; 2005. p. 1–29.
[2] Seals DF, Courtneidge SA. The ADAMs family of metalloproteases: multidomain proteins with multiple functions. Genes Dev 2003;17(1):7–30.
[3] Becherer JD, Blobel CP. Biochemical properties and functions of membrane-anchored metalloprotease-disintegrin proteins (ADAMs). Curr Top Dev Biol 2003;54:101–23.
[4] Moss ML, Jin SL, Milla ME, Bickett DM, Burkhart W, Carter HL, et al. Cloning of a disintegrin metalloproteinase that processes precursor tumour-necrosis factor-alpha. Nature 1997;385(6618):733–6.
[5] Black RA, Rauch CT, Kozlosky CJ, Peschon JJ, Slack JL, Wolfson MF, et al. A metalloproteinase disintegrin that releases tumour-necrosis factor-alpha from cells. Nature 1997;385(6618):729–33.
[6] Blobel CP. ADAMs: key components in EGFR signalling and development. Nat Rev Mol Cell Biol 2005;6(1):32–43.
[7] Prenzel N, Zwick E, Daub H, Leserer M, Abraham R, Wallasch C, et al. EGF receptor transactivation by G-protein-coupled receptors requires metalloproteinase cleavage of proHB-EGF. Nature 1999;402(6764):884–8.
[8] Peschon JJ, Slack JL, Reddy P, Stocking KL, Sunnarborg SW, Lee DC, et al. An essential role for ectodomain shedding in mammalian development. Science 1998;282(5392):1281–4.
[9] Moss ML, Bartsch JW. Therapeutic benefits from targeting of ADAM family members. Biochemistry 2004;43(23):7227–35.
[10] Duffy MJ, Lynn DJ, Lloyd AT, O'Shea CM. The ADAMs family of proteins: from basic studies to potential clinical applications. Thromb Haemost 2003;89(4):622–31.
[11] Mochizuki S, Okada Y. ADAMs in cancer cell proliferation and progression. Cancer Sci 2007;98(5):621–8.
[12] Gomis-Ruth FX. Structural aspects of the metzincin clan of metalloendopeptidases. Mol Biotechnol 2003;24(2):157–202.
[13] Bode W, Gomis-Ruth FX, Stockler W. Astacins, serralysins, snake venom and matrix metalloproteinases exhibit identical zinc-binding environments (HEXXHXXGXXH and Met-turn) and topologies and should be grouped into a common family, the 'metzincins'. FEBS Lett 1993;331(1–2):134–40.
[14] Kuno K, Kanada N, Nakashima E, Fujiki F, Ichimura F, Matsushima K. Molecular cloning of a gene encoding a new type of metalloproteinase-disintegrin family protein with thrombospondin motifs as an inflammation associated gene. J Biol Chem 1997;272(1):556–62.
[15] Porter S, Clark IM, Kevorkian L, Edwards DR. The ADAMTS metalloproteinases. Biochem J 2005;386(Pt 1):15–27.
[16] Blobel CP, Wolfsberg TG, Turck CW, Myles DG, Primakoff P, White JM. A potential fusion peptide and an integrin ligand domain in a protein active in sperm-egg fusion. Nature 1992;356(6366):248–52.
[17] Cho C, Bunch DO, Faure JE, Goulding EH, Eddy EM, Primakoff P, et al. Fertilization defects in sperm from mice lacking fertilin beta. Science 1998;281(5384):1857–9.

[18] Zolkiewska A. Disintegrin-like/cysteine-rich region of ADAM 12 is an active cell adhesion domain. Exp Cell Res 1999;252(2):423–31.
[19] Gaultier A, Cousin H, Darribere T, Alfandari D. ADAM13 disintegrin and cysteine-rich domains bind to the second heparin-binding domain of fibronectin. J Biol Chem 2002;277(26):23336–44.
[20] Iba K, Albrechtsen R, Gilpin B, Frohlich C, Loechel F, Zolkiewska A, et al. The cysteine-rich domain of human ADAM 12 supports cell adhesion through syndecans and triggers signaling events that lead to beta1 integrin-dependent cell spreading. J Cell Biol 2000;149(5):1143–56.
[21] Zigrino P, Steiger J, Fox JW, Loffek S, Schild A, Nischt R, et al. Role of ADAM-9 disintegrin-cysteine-rich domains in human keratinocyte migration. J Biol Chem 2007;282(42):30785–93.
[22] Reddy P, Slack JL, Davis R, Cerretti DP, Kozlosky CJ, Blanton RA, et al. Functional analysis of the domain structure of tumor necrosis factor-alpha converting enzyme. J Biol Chem 2000;275(19):14608–14.
[23] Smith KM, Gaultier A, Cousin H, Alfandari D, White JM, DeSimone DW. The cysteine-rich domain regulates ADAM protease function in vivo. J Cell Biol 2002;159(5):893–902.
[24] Takeda S, Igarashi T, Mori H, Araki S. Crystal structures of VAP1 reveal ADAMs' MDC domain architecture and its unique C-shaped scaffold. EMBO J 2006;25(11):2388–96.
[25] Igarashi T, Araki S, Mori H, Takeda S. Crystal structures of catrocollastatin/VAP2B reveal a dynamic, modular architecture of ADAM/adamalysin/reprolysin family proteins. FEBS Lett 2007;581(13):2416–22.
[26] Takeda S, Igarashi T, Mori H. Crystal structure of RVV-X: an example of evolutionary gain of specificity by ADAM proteinases. FEBS Lett 2007;581(30):5859–64.
[27] Janes PW, Saha N, Barton WA, Kolev MV, Wimmer-Kleikamp SH, Nievergall E, et al. Adam Meets Eph: an ADAM substrate recognition module acts as a molecular switch for Ephrin cleavage in trans. Cell 2005;123(2):291–304.
[28] Gerhardt S, Hassall G, Hawtin P, McCall E, Flavell L, Minshull C, et al. Crystal structures of human ADAMTS-1 reveal a conserved catalytic domain and a disintegrin-like domain with a fold homologous to cysteine-rich domains. J Mol Biol 2007;373(4):891–902.
[29] Mosyak L, Georgiadis K, Shane T, Svenson K, Hebert T, McDonagh T, et al. Crystal structures of the two major aggrecan degrading enzymes, ADAMTS4 and ADAMTS5. Protein Sci 2008;17(1):16–21.
[30] Fox JW, Serrano SM. Structural considerations of the snake venom metalloproteinases, key members of the M12 reprolysin family of metalloproteinases. Toxicon 2005;45(8):969–85.
[31] Takeda S. VAP1: snake venom homolog of mammalian ADAMs. In: Messerschmidt A (Ed.). Handbook of Metalloproteins. John Wiley & Sons, Inc.; 2008, doi:10.1002/0470028637.met234.
[32] Maskos K, Fernandez-Catalan C, Huber R, Bourenkov GP, Bartunik H, Ellestad GA, et al. Crystal structure of the catalytic domain of human tumor necrosis factor-alpha-converting enzyme. Proc Natl Acad Sci U S A 1998;95(7):3408–12.
[33] Orth P, Reichert P, Wang W, Prosise WW, Yarosh-Tomaine T, Hammond G, et al. Crystal structure of the catalytic domain of human ADAM33. J Mol Biol 2004;335(1):129–37.
[34] Shieh HS, Mathis KJ, Williams JM, Hills RL, Wiese JF, Benson TE, et al. High resolution crystal structure of the catalytic domain of ADAMTS-5 (aggrecanase-2). J Biol Chem 2007.
[35] Gomis-Ruth FX, Kress LF, Bode W. First structure of a snake venom metalloproteinase: a prototype for matrix metalloproteinases/collagenases. EMBO J 1993;12(11):4151–7.
[36] Arribas J, Ruiz-Paz S. ADAM17: Regulation of ectodomain shedding. In: Hooper NM, Lendeckel U, editors. The ADAM Family of Proteinases. Dordrecht, The Netherlands: Springer; 2005. p. 171–97.
[37] Gould RJ, Polokoff MA, Friedman PA, Huang TF, Holt JC, Cook JJ, et al. Disintegrins: a family of integrin inhibitory proteins from viper venoms. Proc Soc Exp Biol Med 1990;195(2):168–71.
[38] Calvete JJ, Marcinkiewicz C, Monleon D, Esteve V, Celda B, Juarez P, et al. Snake venom disintegrins: evolution of structure and function. Toxicon 2005;45(8):1063–74.
[39] Lu X, Lu D, Scully MF, Kakkar VV. Structure-activity relationship studies on ADAM protein-integrin interactions. Cardiovasc Hematol Agents Med Chem 2007;5(1):29–42.
[40] Takagi J. Structural basis for ligand recognition by integrins. Curr Opin Cell Biol 2007;19(5):557–64.
[41] Fujii Y, Okuda D, Fujimoto Z, Horii K, Morita T, Mizuno H. Crystal structure of trimestatin, a disintegrin containing a cell adhesion recognition motif RGD. J Mol Biol 2003;332(5):1115–22.
[42] Eto K, Huet C, Tarui T, Kupriyanov S, Liu HZ, Puzon-McLaughlin W, et al. Functional classification of ADAMs based on a conserved motif for binding to integrin alpha 9beta 1: implications for sperm-egg binding and other cell interactions. J Biol Chem 2002;277(20):17804–10.
[43] Gao W, Anderson PJ, Sadler JE. Extensive contacts between ADAMTS13 exosites and von Willebrand factor domain A2 contribute to substrate specificity. Blood 2008.
[44] Alfandari D, Cousin H, Gaultier A, Smith K, White JM, Darribere T, et al. Xenopus ADAM 13 is a metalloprotease required for cranial neural crest-cell migration. Curr Biol 2001;11(12):918–30.
[45] Usami Y, Fujimura Y, Miura S, Shima H, Yoshida E, Yoshioka A, et al. A 28 kDa-protein with disintegrin-like structure (jararhagin-C) purified from Bothrops jararaca venom inhibits collagen- and ADP-induced platelet aggregation. Biochem Biophys Res Commun 1994;201(1):331–9.
[46] Shimokawa K, Shannon JD, Jia LG, Fox JW. Sequence and biological activity of catrocollastatin-C: a disintegrin-like/cysteine-rich two-domain protein from Crotalus atrox venom. Arch Biochem Biophys 1997;343(1):35–43.
[47] Jia LG, Wang XM, Shannon JD, Bjarnason JB, Fox JW. Inhibition of platelet aggregation by the recombinant cysteine-rich domain of the hemorrhagic snake venom metalloproteinase, atrolysin A. Arch Biochem Biophys 2000;373(1):281–6.
[48] Serrano SM, Jia LG, Wang D, Shannon JD, Fox JW. Function of the cysteine-rich domain of the haemorrhagic metalloproteinase atrolysin A: targeting adhesion proteins collagen I and von Willebrand factor. Biochem J 2005;391(Pt 1):69–76.
[49] Serrano SM, Wang D, Shannon JD, Pinto AF, Polanowska-Grabowska RK, Fox JW. Interaction of the cysteine-rich domain of snake venom metalloproteinases with the A1 domain of von Willebrand factor promotes site-specific proteolysis of von Willebrand factor and inhibition of von Willebrand factor-mediated platelet aggregation. FEBS J 2007;274(14):3611–21.
[50] Serrano SM, Kim J, Wang D, Dragulev B, Shannon JD, Mann HH, et al. The cysteine-rich domain of snake venom metalloproteinases is a ligand for von Willebrand factor A domains: role in substrate targeting. J Biol Chem 2006;281(52):39746–56.
[51] Pinto AF, Terra RM, Guimaraes JA, Fox JW. Mapping von Willebrand factor A domain binding sites on a snake venom metalloproteinase cysteine-rich domain. Arch Biochem Biophys 2007;457(1):41–6.
[52] Kamiguti AS, Gallagher P, Marcinkiewicz C, Theakston RD, Zuzel M, Fox JW. Identification of sites in the cysteine-rich domain of the class P-III snake venom metalloproteinases responsible for inhibition of platelet function. FEBS Lett 2003;549(1–3):129–34.
[53] Morita T. Structures and functions of snake venom CLPs (C-type lectin-like proteins) with anticoagulant-, procoagulant-, and platelet-modulating activities. Toxicon 2005;45(8):1099–114.

■■ 総合論文 ■■

血管細胞の破壊毒素：明らかになったADAM型細胞表面プロテアーゼの構造*

荒木聡彦*，五十嵐智子**，武田壮一**

1. はじめに

細胞と外界とのシグナルのやりとりは，多細胞生物である人間にとって，細胞間のシグナル伝達や，細胞と体液・間質との間のシグナル伝達などを含め，生物を成り立たせるための源であり，生物活動のための源でもある。細胞が外界とシグナルをやりとりする時には，シグナル分子タンパク質などの細胞表面のタンパク質がお互いに結合，修飾，切断し合うことによって，シグナルの状態を確定し情報伝達する。この中で，細胞表面のタンパク質切断による情報伝達は，広く起こっているにもかかわらず，まだあまりよく分かっていない分野である。しかし，生物で重要なシグナル伝達の分野であることに加え，アルツハイマー病やぜんそくなど様々な病態への関与も明らかになりつつあり，医学的な重要性から非常にホットに研究が進められている[1,2]。出血性ヘビ毒素も，細胞表面タンパク質切断酵素の一種である[3]。今まで，細胞膜上にあるこれらの酵素は研究が難しかったが，ヘビ出血毒素を用いることで最近いくつかの研究の進展があった。マムシ，ハブ，ガラガラヘビなどの代表的な多くのヘビ毒が出血毒なのであるが，このような毒素がどのようにして出血に至らしめるかは実は全く未知である。それは一般的な細胞表面タンパク質分解機構とそれに伴うシグナル伝達の仕組みそのものが，そもそもまだあまり解っていないからである。ヘビ出血毒素による出血機構解明とともに細胞表面タンパク質の分解機構の解明が進むことによって，多くの細胞間シグナル伝達が関与する生物のしくみが飛躍的に明らかになるかもしれない。そこで今回進展があったADAM型の細胞表面タンパク質分解酵素について概説する。

2. 全く解っていない表面タンパク質切断機構

細胞膜上にあるシグナル受容タンパク質や接着タンパク質の切断や除去をになう細胞膜プロテアーゼは，細胞膜上のシグナル伝達制御に欠かすことができない。現在，ヒトを含め多くの

---

* The crystal structure of the hemorrhagic snake venom toxin reveals the molecular architecture of the ADAM family cell-surface proteinases.

* Satohiko ARAKI　名古屋大学大学院理学研究科附属臨海実験所
Sugashima Marin Biological Laboratory, Graduate School of Science, Nagoya University
〒517-0004　三重県鳥羽市菅島町429-63
** Tomoko IGARASHI and Soichi TAKEDA　国立循環器病センター研究所心臓生理部
Department of Cardiac Physiology, National Cardiovascular Center Research Institute
〒565-8565　大阪府吹田市藤白台5-7-1

Key words: Cell surface proteolysis, ADAM proteinase, snake venom toxin, apoptosis, vascular endothelial cell

生物において，そのような細胞膜タンパク質を切断するプロテアーゼとして，フリン様プロテアーゼ，ADAM型プロテアーゼ，ガンマセクレターゼなどが知られている[4]。中でもとくにADAM型プロテアーゼは，その活動がシグナル伝達過程に伴って起き，細胞表面で最初に起こる切断であることから (図 1)，切断を伴うシグナル伝達機構解明に必須であると思われるが，どのように制御されており，どのように標的を認識するのか，全く解っていない[5]。その理由の一つに，ADAM型プロテアーゼはジスルフィド結合を多く含み細胞外タンパク質独特の構築原理を持っているため大腸菌等によるリコンビナントタンパク質の合成が難しく，研究がしにくいことが挙げられる。そこで唯一，天然活性を持って大量に得て研究することのできるADAM型プロテアーゼが，ヒト分子も含めた多くのADAMの中で，出血性ヘビのADAM型毒素なのである。

3. ヘビ毒素による血管内皮細胞の破壊

3.1 出血性ヘビ毒素

ヘビ毒液中に含まれる多様な毒素は，細胞膜表面の種々の分子に作用し，細胞の機能を阻害・制御することが知られている[6]。ヘビ毒はその特異性から，細胞膜機能や細胞膜分子の研究に大きな貢献をしてきた。コブラ毒などに含まれる神経作用ヘビ毒素は細胞膜イオンチャネルに作用することからこれを用いてイオン輸送の研究が進展してきた。他方，ガラガラヘビ毒，マムシ毒，ハブ毒などは出血性ヘビ毒であり，出血毒素や，止血阻害毒素を多く含有している。以前より止血阻害毒素の方は，血小板凝集レセプターや凝固因子 (フィブリノーゲンなど) に作用することから血液凝固の研究や臨床に用いられてきた[7](図 2)。一方，出血毒のほうは，あまり研究が進んでおらず，ADAM型プロテア

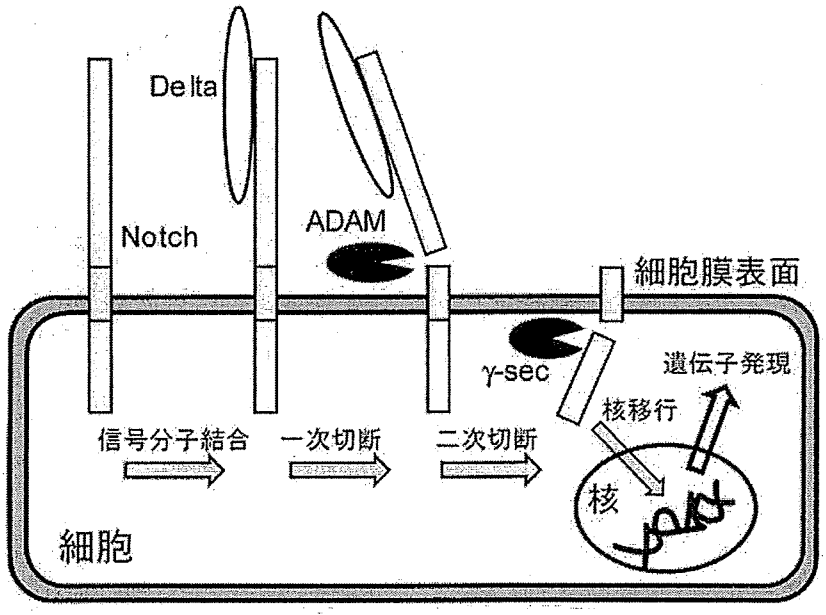

図 1　細胞表面タンパク質の切断とシグナル伝達
細胞表面シグナル分子であるNotchは，細胞シグナル分子Deltaと結合すると，ADAMによる一次切断，γセクレターゼによる二次切断の順に切断され，細胞内部分が核に移行して遺伝子発現を誘導する。同様に他の多くの細胞表面分子はシグナルに際して切断を受け，情報伝達に関与する。

ーゼであることが解っている程度で，その標的も，制御機構も現在解っていない。

3.2 出血毒素の標的

出血毒素の標的については，ADAM型プロテアーゼがメタロプロテアーゼの仲間であるため，コラーゲンを分解できる仲間も多いことから，血管の基底膜を構成するコラーゲンを標的としてこれを分解することが出血に至る主因ではないかとも考えられているが，いまだに確証は得られていない (図 2)。また，コラーゲン分解が目標なら，なぜコラーゲン分解酵素であるマトリックスメタロプロテアーゼ (MMP) 型ではなく，細胞表面タンパク質分解酵素の ADAM 型であるのかも不思議で，議論になっている[8]。確証が得られないのは，多くの出血プロテアーゼは一度に色々なタンパク質を切る能力を持っており特異性が低いため，主因の標的が特定しづらいということにも因る。その中で，VAP1という出血毒素は，基質特異性が高く，他の出血毒素が分解する多くのタンパク質を分解しないため，副作用が少なく出血の標的研究に用いやすい[9),10)]。興味深いことは，VAP1 はコラーゲン分解活性がないのに出血活性があることである。

3.3 アポトーシス誘導毒素

VAP1 を含む VAP (Vascular Apoptosis-Inducing Protein) ファミリーの毒素は，アポトーシス誘導毒素として見出されたもので，血管内皮細胞に強力なアポトーシス (能動的細胞死) を引き起こす性質をもっている[9)] (図 3)。言い換えれば，これらの毒素は，血管内皮細胞に対して自殺のスイッチを外から起動させて，血管細胞を殺す

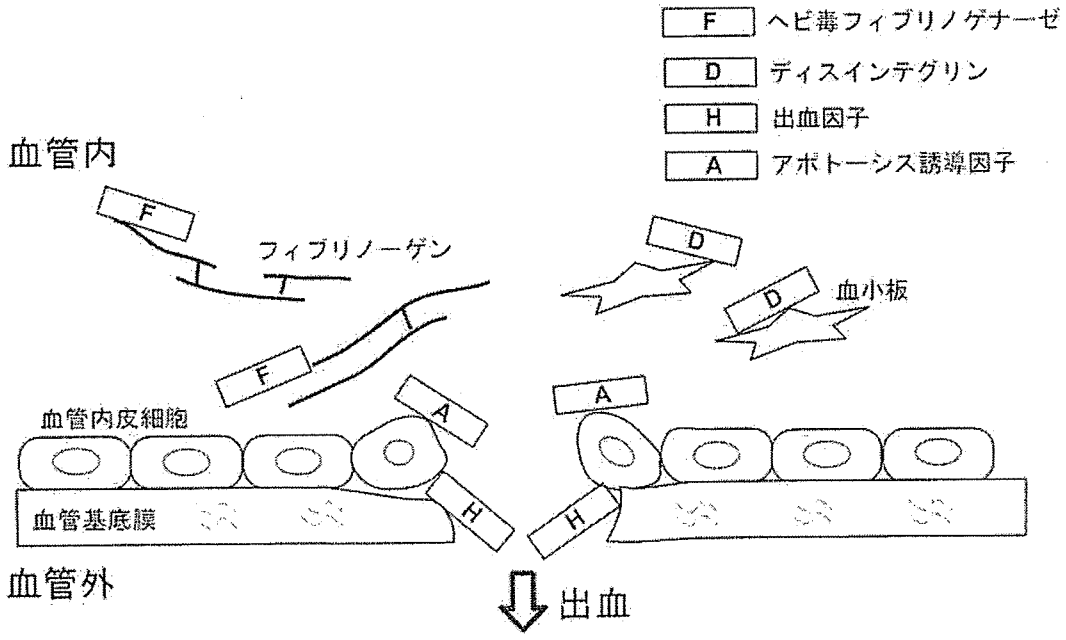

図 2 ヘビ毒素群と出血機構のモデル図
ヘビ毒は複数の毒素から構成されており，止血阻害毒素としては，ヘビ毒フィブリノゲナーゼがフィブリノーゲンを無力化したり，ディスインテグリンが血小板レセプターを阻害したりして血液凝固による止血を阻害する。出血性プロテアーゼなどの出血毒素の標的はまだあまり分かっておらず，基底膜コラーゲンや血管内皮細胞などが候補として上がっている。

ことができる。これらは，繊維芽細胞や平滑筋細胞などは殺さず血管内皮細胞を殺す特異性を持っている。またこのような毒素が引き起こすアポトーシスは非常に特徴的で，他のアポトーシスよりも強く細胞を粉々に分裂させる特徴(細胞断片化作用)をもっている[11),12)](図3C，E)。

3.4 ヘビ毒素による強い細胞断片化

細胞断片化は，細胞膜表面が胞子状に突出してつぶつぶを作り，最後には細胞全体が葡萄状になって粉々に分裂するものである。この作用はアポトーシスの実行因子である細胞内プロテアーゼ(カスパーゼ)に依存的で，カスパーゼを阻害すると毒素による細胞死は起こるものの強い細胞断片化は起こらない[11)](図3D)。したがって強い細胞断片化はヘビ毒プロテアーゼによる直接分解によるものではなく，ヘビ毒の引き起こすアポトーシスシグナルがカスパーゼを活性化することによって生じるものであり，特別なアポトーシスの一形態であると考えられる。このヘビ毒素は，このような特異な現象を血管細胞に引き起こす，シグナル誘導タンパク質であると言える。この特異なシグナル誘導タンパク質はいったいどのようにして，細胞に働きかけるのだろうか。この毒素タンパク質の構造が，そのヒントを与えてくれると考えられるが，この毒素はADAM型といわれるドメイン構造を持っている[13),14)]。

4. ADAM型プロテアーゼ

4.1 ADAM

ADAM型プロテアーゼの「ADAM」とはA Disintegrin And Metalloproteaseの頭文字をとったもので，「ディスインテグリンドメインとメタ

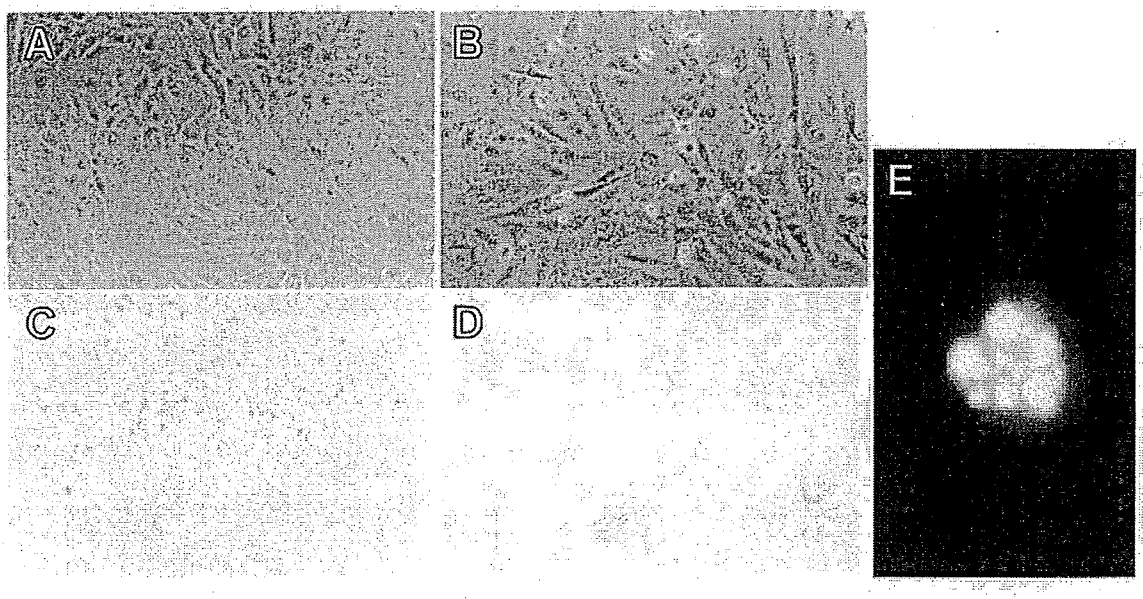

図3 血管細胞アポトーシス誘導毒素VAP1による細胞死
Aは通常の培養血管内皮細胞。血清除去などによる血管細胞死(B)は細胞が丸い状態になり，あまり細胞断片化は起こらないが，VAP1による細胞死(C，E)は強い細胞断片化が起こる。この断片化はカスパーゼ阻害剤によって阻止され，その結果Bと似た形態の細胞死が生じる(D)。(A～D：位相差顕微鏡像(×100)，E：核染色による蛍光顕微鏡像(×400))

ロプロテアーゼドメインを持ったタンパク質ファミリー」のことを指している[15]。ADAMファミリーは，ヒトでは24種類のADAMがある。しかし，それぞれがどのような標的を切断するのか，どのような機能を担っているのかはよく分かっていない[5]。ADAMタンパク質は，ヒトにおいて多くの病気との関係が研究されている。ADAM33はぜんそくの関連遺伝子と推定され，ADAM12は心臓疾患に関与するが，どのようなしくみで関わるのか詳細は分かっていない[1),2)]。

アミノ酸配列から推定される構造は図のように，メタロプロテアーゼドメイン，ディスインテグリンドメイン，システインリッチドメインが順に並んでいる(図4)。ディスインテグリンドメインとは，細胞接着因子であるインテグリンを阻害するヘビ毒素であるディスインテグリンに由来している(図4)。ADAMというネーミングはしたがって，「インテグリン阻害タンパク質に似たドメインを持つメタロプロテアーゼ」という意味合いになっている。そこでADAMが，本当にディスインテグリンと同様なインテグリン結合活性および結合様式をもつのかどうかに，興味がもたれていた。

システインリッチドメインは名前の通りシステイン残基を多く含み，これらはほとんどジスルフィド結合の形成に寄与していると考えられるが，機知のアミノ酸配列との相同性が無く，どのような機能をするかよく分かっていない。

4.2 ADAMの4つの謎

細胞表面タンパク質切断酵素ADAMは，まず①標的認識機構が分からない。別の表面タンパク質切断酵素であるフリンは，標的タンパク質中の連続した塩基性アミノ酸部位を認識してその近傍を切断する。しかし，ADAMは，標的タンパク質群に共通したアミノ酸配列などが見つからない。どのような基準で標的を選んでいるのかが分からないのである[5]。第二に②活

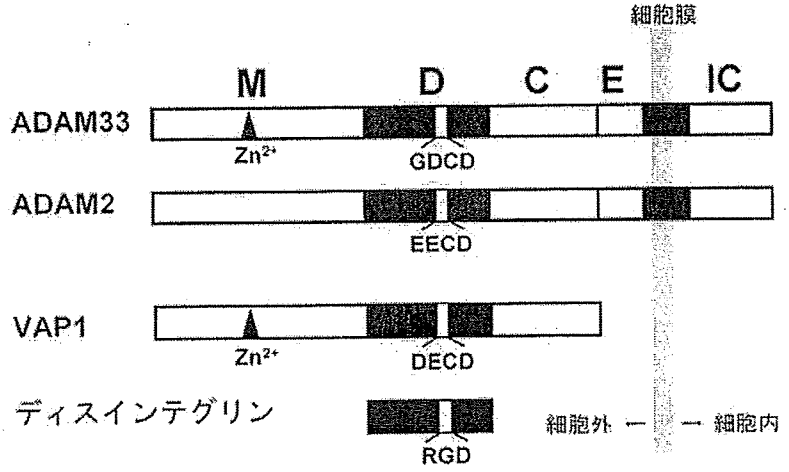

図4 ADAMの一次構造
ADAMファミリーはメタロプロテアーゼ(M)ドメイン，ディスインテグリン(D)ドメイン，システインリッチ(C)ドメインの基本構造を持ち，細胞膜結合型はその後にEGF(E)ドメイン，細胞膜貫通領域，細胞内(IC)ドメインを持っている。Mドメインには亜鉛結合によるプロテアーゼ活性を持つものと持たないものがある。ディスインテグリンは細胞接着タンパク質であるインテグリンに結合しうるRGD配列を有する。ADAMはディスインテグリンに類似のDドメインを持つが，RGDとは異なるアミノ酸配列をもつ。この異なる配列を持つADAMのディスインテグリンループ部が，インテグリン類に直接結合するかどうか興味が持たれていた。

性化機構が分からない。フリンは，細胞表面に出てきた候補タンパク質を全て分解するため，主にタンパク質を最終形に成熟させるためのタンパク質分解に用いられると考えられている。それに対しADAMは細胞シグナルが働いたときや細胞刺激が与えられたときにタンパク質分解を引き起こすと考えられているが，どのような機序で切断が引き起こされるのか，制御方式が分からないのである(図1)。さらに第三に，③ADAMのうちの半数は活性部位のアミノ酸が置換しているためプロテアーゼ活性を原理的に持たないのに，形だけメタロプロテアーゼの形を持っている(図4，ADAM2)。この，活性を持たないメタロプロテアーゼ様構造が何の役に立っているかが分からないのである。そして第4に，④ADAMのディスインテグリンループ(ADAMではさまざまな配列を持っ：GDCDやDECDなど(図3))が，ディスインテグリンのRGD配列のようにインテグリンを標的として結合するのかどうか，であり，そしてそれがADAMの主標的や副標的なのかどうか，と言う点である。

5. 明らかになったADAMの基本構造

5.1 VAP1の構造

このような細胞表面タンパク質分解酵素ADAMがどのように基質を見分け切断するかを解明するために，ガラガラヘビ由来アポトーシス毒素VAP1を用いてX線結晶解析をし，ADAMの立体構造を初めて解明することができた[16),17)]。

VAP1の構造は図4のようになっていた。VAP1は2量体であるが，これは1量体部分を表

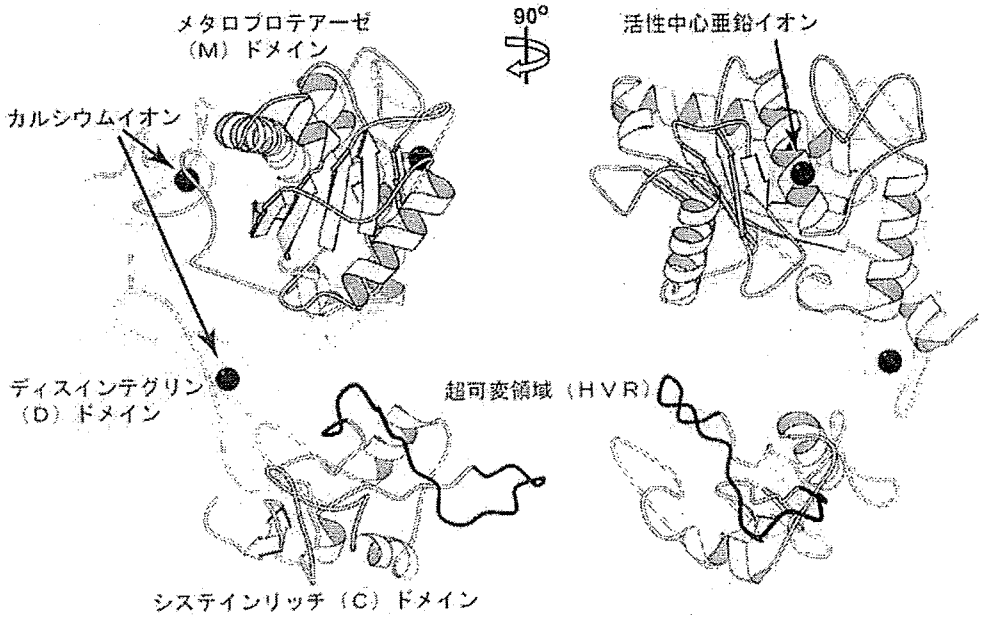

図5 VAP1の立体構造
ADAMの基本骨格構造がVAP1の結晶解析によって初めて解かれた。右は90℃横から見た図。メタロプロテアーゼドメイン，ディスインテグリンドメイン，システインリッチドメインはアルファベットのC型の配置をしている。C型のアーム部分であるDドメインはカルシウムイオンと多数のジスルフィド結合によって堅い構造になっている。濃線の超可変領域(HVR)は，プロテアーゼ活性中心である亜鉛イオン部と相対している。

している。また他の1量体ADAM型毒素VAP2も同様な構造をしていることが分かった[18]。VAP1はADAMの基本構造であるメタロプロテアーゼドメイン(M)，ディスインテグリンドメイン(D)，システインリッチドメイン(C)から成っており，図のようにMDC各ドメインがアルファベットのC型に湾曲した配置をとる構造をしていた。

C末端はC・Dドメインの境界にあり，ADAMにおいては細胞膜に連結している箇所である。ここを基準にすると，C型構造の構造的両末端は，一つはDドメインを経由してメタロプロテアーゼのZn^{2+}を配位した触媒活性中心であり，もう一方はCドメインの頂点の超可変領域(HVR)と記した部分(図5濃線)になる。この時，プロテアーゼ活性中心亜鉛イオン(Zn^{2+})部とHVR部は対面した形となる。このHVR部は，各ADAMを比較してアミノ酸配列の保存性が低く，また，長さや予測される立体構造においてもバリエーションが特別に高い部分であることから，超可変領域(Hyper Variable Region：HVR)と名付けた。各ADAMを特徴付けるHVRと，切断活性部分が対面していることは，切断標的の選択に寄与していることを強く示唆している。

5.2 ディスインテグリンループ

ディスインテグリンドメインは，ディスインテグリン単体分子とは違って，2個のCa^{2+}を配位して堅いアーム構造を作っており，ADAM全体のC型構造の支柱を成している(図5)。ディスインテグリン単体分子では，先端のディスインテグリンループにあるアミノ酸配列RGD(図6トリメスタチンの濃線)が細胞接着分子インテ

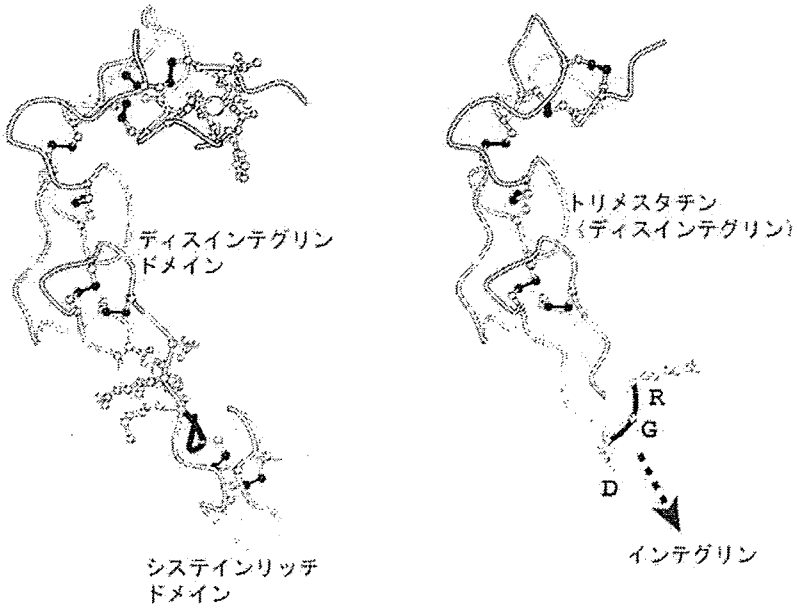

図6 ディスインテグリンドメイン
ADAMのディスインテグリンドメインは，既に立体構造が判明していたディスインテグリン単体分子(トリメスタチンなど)を内包する形になっている。しかし，濃線のディスインテグリンループは，ADAMではシステインリッチドメインに埋め込まれ，インテグリン結合には寄与できない。

グリンに結合する部位である。これに対しADAMのディスインテグリンドメインはRGDCDやDECDなど異なる配列を持つ。しかし，この部分のペプチドのみを合成するとインテグリンと結合可能であることなどから，やはりインテグリンとの結合部位ではないかと期待されていた[5]。しかし今回明らかにされた立体構造では，ADAMのディスインテグリンループ(図6ディスインテグリンドメインの濃線の部分)はCドメインを配置するのに用いられており，タンパク質表面に露出していないため，残念ながら標的分子への結合には関与しないことが示唆された。

5.3 ADAMファミリーの各分子の構造比較

ぜんそくや心臓疾患に関与するとされたADAM33やADAM12も含め，今回の立体構造解明で明らかになった構造的に重要な部分の配列は，全てのADAMファミリー分子間で一致していた。したがって，他のADAMも，今回明らかになったVAP1の構造と同じ構築原理を有していると考えられる。このことはプロテアーゼ活性配列を失っている半数のADAMについても同様で，ディスインテグリンアームのCa配位を始めとして構造は全く等しいと考えられた。ADAMでそれぞれ違っている部分は，Zn結合部近くの触媒部付近が少し異なることの他は，超可変領域HVRの部分だけであった。そしてこのバリエーションが特別に高いHVR部位がADAM構造のC型構造突端にあることから，各ADAMの役割の違いを最も決定付けるものは，そこに結合する分子によってなされていると考えられた。

5.4 表面タンパク質切断のしくみへ

立体構造が分かったことで，いくつかのADAMの謎の闇から，表面タンパク質切断のしくみ解明へ近づくことができた。① ADAM標的については，ADAMファミリーの中で各ADAMを特徴付ける部分が，突出部位であるHVRであることが分かったため，ここに結合するものが切断を受ける標的か標的選択に重要な分子であることが予想された(図7)。② 活性化機構については，HVRが標的選択に関するものであれば，その結合分子が各ADAMの活性化に関与するであろう。また，特徴的な構造であることから，C型湾曲構造も活性化に関与しそうなことが伺われる。③メタロプロテアーゼ活性を持たないADAMは，成熟の過程でMドメイン・Dドメインが切り出されることも多い[5]。したがってM，Dを失ったあと，立体構造の頂点であるHVR部位が，特定蛋白質結合のレセプターとして機能を発揮することが予想された。

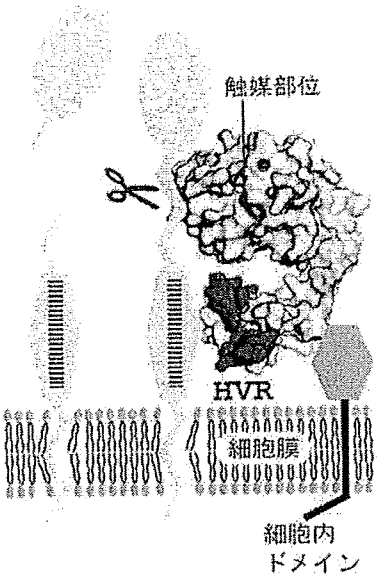

図7 ADAMによる表面タンパク質切断モデル
今回判明したADAMの基本構造から，ADAMは細胞表面においてこのモデルのような分子形態で細胞膜上に存在していると考えられる。各ADAMの違いは超可変領域(HVR)であることから，ここに結合する分子によって，切断をする標的が選別される可能性が強く示唆される。

しかし，だとしても，なぜ不活性のMドメイン・Dドメインが未成熟のADAMに必要なのかは分からない。特徴的な湾曲構造全体が成熟の過程に必要な可能性が考えられる。④従来関与が期待されていたADAMのディスインテグリンループは，タンパク質表面に無いため，標的結合には関与しないことが強く示唆された。しかし，このディスインテグリンドメイン全体のアーム構造は，特徴的なC型構造の支柱部分を形成しており，活性化に重要な役割を果たすことが期待される。

6. おわりに

今回，出血毒素VAP1の立体構造が解明されることによって，細胞表面タンパク質切断酵素ADAMファミリー全体の基本構造が明らかになった。今後，HVRの標的分子などが見つけ出されることによって，出血機構のみならず，一般的な表面タンパク質切断のしくみが徐々に明らかにされていくことが期待される。それらは，ぜんそくやアルツハイマー病などのしくみの解明などにつながり，また細胞表面のしくみの解明から生物への理解と応用が一段と進むかもしれない。

生命科学の領域はタンパク3000プロジェクトに代表される網羅的タンパク質構造解析の著しい進展により新たな局面を迎えている。すなわち，さまざまな生命現象にかかわる高分子の立体構造と機能の相関が当たり前のように原子レベルの分解能で議論できる時代になってきた。本稿はその一例でもある。タンパク質の立体構造の知見が基礎生物学・医学領域への貢献に留まらず，今後は材料化学など異分野との融合によりさまざまな境界領域のサイエンスを生み出していく可能性が期待される。

参考文献

1) P. Van Eerdewegh, R. D. Little, J. Dupuis, R. G. Del Mastro, K. Falls, J. Simon, D. Torrey, S. Pandit, J. McKenny, K. Braunschweiger, A. Walsh, Z. Liu, B. Hayward, C. Folz, S. P. Mannmg, A. Bawa, L. Saracino, M. Thackston, Y. Benchekroun, N. Capparell, M. Wang, R. Adair, Y. Feng, J. Dubois, M. G. FitzGerald, H. Huang, R. Gibson, K. M. Allen, A. Pedan, M. R. Danzig. S. P. Umland, R. W. Egan, F. M. Cuss, S. Rorke, J. B. Clough, J. W. Holloway, S. T. Holgate and T. P. Keith, Association of the ADAM33 gene with asthma and bronchial hyperresponsiveness, *Nature*, **418**, 426-430 (2002).
2) T. M. Allinson, E. T. Parkin, A. J. Turner and N. M. Hooper, ADAMs family members as amyloid precursor protein alpha-secretases, *J. Neurosci. Res.*, **74**, 342-352 (2003).
3) L. A. Hite, L. G. Jia, J. B. Bjarnason and J. W. Fox, cDNA sequences for four snake venom metalloproteinases : structure, classification, and their relationship to mammalian reproductive proteins, *Arch. Biochem. Biophys.*, **308**, 182-191 (1994).
4) M. E. Carlson and I. M. Conboy, Regulating the Notch pathway in embryonic, adult and old stem cells, *Curr. Opin. Pharmacol.*, **7**, 303-309 (2007).
5) S. Mochizuki and Y. Okada, ADAMs in cancer cell proliferation and progression, *Cancer. Sci.*, **98**, 621-628, (2007).
6) Q. Lu, J. M. Clemetson and K. J. Clemetson, Snake venoms and hemostasis, *J. Thromb. Haemost.*, **3**, 1791-1799 (2005).
7) J. White, Snake venoms and coagulopathy, *Toxicon*, **45**, 951-967 (2005).
8) J. W. Fox and S. M. Serrano, Structural considerations of the snake venom metalloproteinases, key members of the M12 reprolysin family of metalloproteinases, *Toxicon*, **45**, 969-985 (2005).

9) S. Araki, T. Ishida, T. Yamamoto, K. Kaji and H. Hayashi, Induction of apoptosis by hemorrhagic snake venom in vascular endothelial cells, *Biochem. Biophys. Res. Commun.*, **190**, 148-153 (1993).
10) S. Araki, S. Masuda, H. Maeda, J. Y. Miao and H. Hayashi, Involvement of specific integrins in apoptosis induced by vascular apoptosis-inducing protein 1, *Toxicon*, **40**, 535-42 (2002).
11) J. Maruyama, H. Hayashi, J. Y. Miao, H. Sawada and S. Araki, Severe cell fragmentation in the endothelial cell apoptosis induced by snake apoptosis toxin VAP1 is an apoptotic characteristic controlled by caspases, *Toxicon*, **46**, 1-6 (2005).
12) S. Araki, Y. Shimada, K. Kaji and H. Hayashi, Apoptosis of vascular endothelial cells by fibroblast growth factor deprivation, *Biochem. Biophys. Res. Commun.*, **168**, 1194-1200 (1990).
13) S. Masuda, T. Ohta, K. Kaji, J. W. Fox, H. Hayashi and S. Araki, cDNA cloning and characterization of vascular apoptosis-inducing protein 1, *Biochem. Biophys. Res. Commun.*, **278**, 197-204 (2000).
14) S. Masuda, H. Hayashi, H. Atoda, T. Morita and S. Araki, Purification, cDNA cloning and characterization of the vascular apoptosis-inducing protein, HV1, from Trimeresurus flavoviridis, *Eur. J. Biochem.*, **268**, 3339-3345 (2001).
15) T. G. Wolfsberg, P. Primakoff, D. G. Myles and J. M. White, ADAM, a novel family of membrane proteins containing A Disintegrin And Metalloprotease domain : multipotential functions in cell-cell and cell-matrix interactions, *J. Cell Biol.*, **131**, 275-278 (1995).
16) T. Igarashi, Y. Oishi, S. Araki, H. Mori and S. Takeda, Crystallization and preliminary X-ray crystallographic analysis of the two vascular apoptosis-inducing proteins (VAPs) from Crotalus atrox venom, *Acta Cryst. F*, **62**, 688-691 (2006).
17) S. Takeda, T. Igarashi, H. Mori and S. Araki, Crystal structures of VAP1 reveal ADAMs' MDC domain architecture and its unique C-shaped scaffold, *EMBO J.*, **25**, 2388-2396 (2006).
18) T. Igarashi, S. Araki, H. Mori and S. Takeda, Crystal structures of catrocollastatin/VAP2B reveal a dynamic, modular architecture of ADAM/adamalysin/reprolysin family proteins, *FEBS Lett.*, **581**, 2416-2422 (2007).

the FEBS Journal

Functional importance of charged residues within the putative intracellular loops in pH regulation by Na^+/H^+ exchanger NHE1

Takashi Hisamitsu*, Keiji Yamada*, Tomoe Y. Nakamura and Shigeo Wakabayashi

Department of Molecular Physiology, National Cardiovascular Center Research Institute, Suita, Japan

Keywords
charge-reversal mutation; Na^+/H^+ exchanger; pH regulation; surface labeling; transport kinetics

Correspondence
S. Wakabayashi, Department of Molecular Physiology, National Cardiovascular Center Research Institute, Suita, Osaka 565-8565, Japan
Fax: +81 6 6835 5314
Tel: +81 6 6833 5012
E-mail: wak@ri.ncvc.go.jp

*These authors contributed equally to this work

(Received 13 February 2007, revised 21 June 2007, accepted 28 June 2007)

doi:10.1111/j.1742-4658.2007.05962.x

The plasma membrane Na^+/H^+ exchanger 1 is activated in response to various extrinsic factors, and this process is regulated by an intracellular pH-sensing mechanism. To identify the candidate residues responsible for intracellular pH regulation, we analyzed the functional properties of engineered Na^+/H^+ exchanger 1 mutants with charge-reversal mutations of charged residues located in the intracellular loops. Na^+/H^+ exchanger 1 mutants with mutations at 11 positions were well expressed in the plasma membrane, but that with E247R was not, suggesting that Glu247 is important for the functional expression of Na^+/H^+ exchanger 1. Charge-reversal mutations of Glu131 (E131R, E131K) and Arg327 (R327E) resulted in a shift in the intracellular pH dependence of the exchange activity measured by $^{22}Na^+$ uptake to the acidic side, and it abolished the response to growth factors and a hyperosmotic medium; however, mutations of Asp448 (D448R) and Arg500 (R500E) slightly shifted it to the alkaline side. In E131R, in addition to the change in intracellular pH dependence, the affinities for extracellular Na^+, Li^+ and the inhibitor 5-(*N*-ethyl-*N*-isopropyl)amiloride significantly increased. Furthermore, charge-conserved mutation of E131 (E131D) was found to have no effect, whereas charge neutralization (E131Q) resulted in a slight acidic shift of exchange. These results support the view that the multiple charged residues identified in this study, along with several basic residues reported previously, participate in the regulation of the intracellular pH sensing of Na^+/H^+ exchanger 1. In addition, Glu131 may also be important for cation transport.

Na^+/H^+ exchangers (NHEs) belong to a solute carrier family (SLC9) that is involved in catalyzing the electroneutral exchange of Na^+ and H^+ and regulating pH homeostasis, cell volume, and transepithelial Na^+ absorption [1–6]. Various extrinsic factors, including hormones, growth factors, pharmacologic agents, and mechanical stimuli, control the activity of the ubiquitous exchanger isoform NHE1 [1–6]. NHE1 activation is occasionally a risk factor involved in the pathogenesis of various diseases. For example, it plays a critical role in the onset of cardiac hypertrophy and heart failure during ischemia and reperfusion, as confirmed by the significant reduction in heart damage observed on administration of NHE1-specific inhibitors [7,8]. Various extrinsic factors have been shown to enhance NHE1 activity by shifting the intracellular pH (pH_i) dependence of the Na^+/H^+ exchange to the alkaline side, and this is presumed to occur via interactions between regulatory factors and the cytoplasmic domain of NHE1 and/or by the post-translational

Abbreviations
EIPA, 5-(*N*-ethyl-*N*-isopropyl)amiloride; HA, hemaglutinin; IL, intracellular loop; NHE, Na^+/H^+ exchanger; NHS-LC-biotin, succinimidyl-6-(biotinamide)hexanoate; pH_i, intracellular pH; TM, transmembrane-spanning region.

modification of NHE1 or its accessory factors. This phenomenon is usually explained by the assumption that NHE1 possesses an allosteric regulatory site for intracellular protons that is distinct from the Na^+ or H^+ transport site, and that external stimuli increase the H^+ affinity of this H^+-regulatory site [1,9–11].

Members of the NHE family possess similar general structures, comprising a C-terminal cytoplasmic regulatory domain (~ 300 amino acids) and an N-terminal transmembrane domain (~ 500 amino acids) that contains 12 membrane-spanning segments [1–3]. In the plasma membrane, NHE1 is known to exist as a dimer [12,13], and our recent study provided evidence that dimerization is essential for this molecule to maintain physiologic pH_i sensitivity [14]. We previously demonstrated that deletion of the cytoplasmic subdomains of NHE1 shifted the pH_i dependence of the Na^+/H^+ exchange either to the acidic or the alkaline side [15], implying the importance of the cytoplasmic domain in regulating pH sensitivity. Recently, we also presented evidence that calcineurin homologous protein, an obligatory binding partner of NHE1, is one of the key molecules involved in regulating pH sensitivity [16–18]. Furthermore, we [19] and others [20] reported that mutation of Arg residues, namely Arg440 in intracellular loop 5 (IL5) and Arg327 in IL4, largely shift the pH_i dependence of the exchange to the acidic side. These latter observations raised the interesting possibility that a cluster of charged residues in the ILs along with the calcineurin homologous protein-bound cytoplasmic subdomain may regulate the function of NHE1 as a pH sensor. In this study, in order to further identify the critical residues responsible for regulating pH sensitivity, we analyzed the effect of charge-reversal mutation of charged residues in putative ILs or in transmembrane-spanning region (TM)/IL boundaries on the kinetics of the Na^+/H^+ exchange. Of the 12 mutations examined in this study, we identified Glu131 in IL1 as an important residue involved in regulating pH_i sensitivity and Na^+ transport.

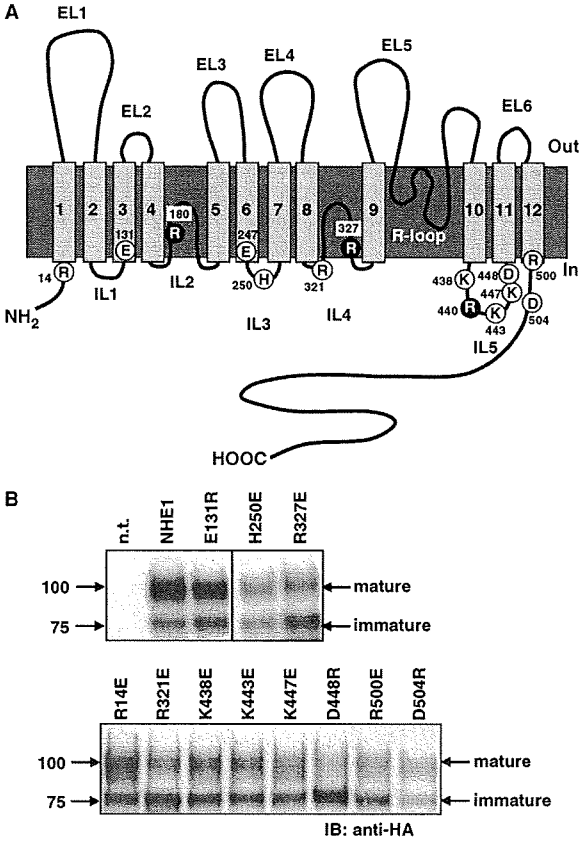

Fig. 1. Expression of charge-reversal mutant NHE1s. (A) Secondary structure model of NHE1. Relative positions of engineered residues are indicated in the figure. R-loop, re-entrant loop. Arg440 [19] and Arg327 and Arg180 [20] were previously reported to be critical residues responsible for pH_i dependence of NHE1. (B) Immunoblot of proteins obtained from cells stably expressing the wild-type or other mutant NHE1s. Cell lysate proteins (20 μg per lane) were subjected to 3–8% SDS/PAGE and immunostained with antibody to HA. n.t., nontransfected PS120 cells.

Results

In this study, we focused on the mutation of charged residues in the intracellular loops of NHE1. Figure 1A shows the previously reported membrane topology model of human NHE1 [22]. As the first search, we introduced charge-reversal mutations (Arg, Lys or His to Glu, Glu or Asp to Arg) in 12 charged residues, namely: Arg14 in the N-tail; Glu131 in IL1; Glu247 and His250 in IL3; Arg321 and Arg327 in IL4; Lys438, Lys443, Lys447 and Asp448 in IL5; and Arg500 and Asp504 in the C-tail of hemaglutinin (HA)-tagged NHE1. We transfected expression vectors carrying these individual NHE1 point mutants into NHE-deficient PS120 cells and selected the population of cells expressing the NHE variants by activity-dependent selection procedures, i.e. by H^+-killing selection [23]. Of the 12 different mutants, E247R was not expressed, indicating that the substitution of Glu247 with Arg causes a severe functional defect (catalytic inactivity and/or a membrane-expression defect) in the NHE1 molecule. The other 11 NHE1 mutants were well expressed in PS120 cells, as observed in the immunoblot analysis (Fig. 1B). First, we assessed the surface expression of these mutant NHEs by surface biotinylation. To semiquantitatively evaluate this surface expression, we estimated the

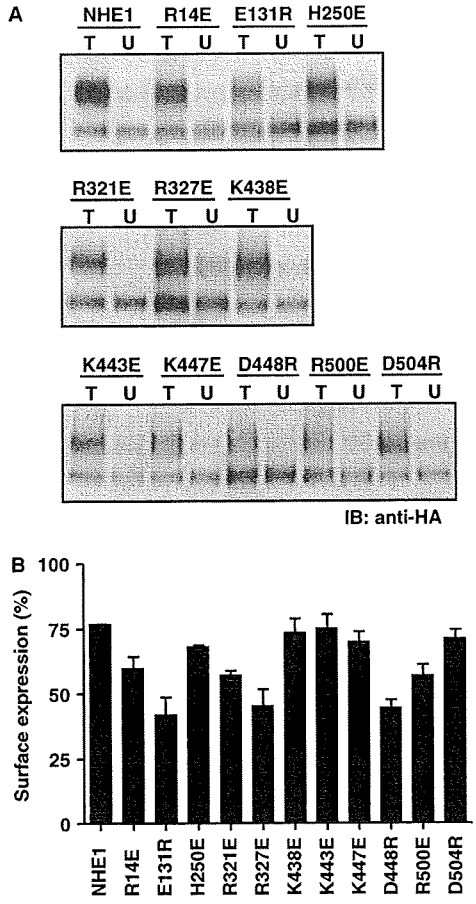

Fig. 2. Surface biotin labeling of various NHE1 variants. (A) Cells expressing various NHE1 variants were treated with 1 mM NHS-LC-biotin, and the cell lysate was incubated with streptavidin-agarose beads. An aliquot of cell lysates before (total, T) and after (unbound, U) incubation with beads was subjected to immunoblot analysis with an antibody to HA. (B) Density of mature and immature protein bands was measured by densitometric scanning and determining the amount of NHE1 proteins absorbed to streptavidin-agarose beads by subtracting the amount of unbound NHE1 from that of total NHE1 (including all four forms of NHE1). Data are represented as a percentage of bead-bound NHE1.

amount of NHE1 protein adsorbed onto streptavidin-agarose beads by subtracting the amount of unbound NHE1 (including immature NHE1) from the amount of total mature NHE1 expressed (Fig. 2A). On the basis of this analysis, we concluded that approximately 75% of the total wild-type NHE1, including the nonspecifically bound proteins that accounted for 5–10%, were adsorbed onto the beads, i.e. expressed on the cell surface (Fig. 2B). Charge-reversal mutations did not alter the surface expression of NHE1 to a large extent, except for the mutations of Glu131, Arg327, and Asp448, which slightly reduced it (Fig. 2B). Essentially the same results were obtained using two different batches of cell populations derived from different transfectants.

Next, we measured the pH_i dependence of the 5-(*N*-ethyl-*N*-isopropyl)amiloride (EIPA)-inhibitable $^{22}Na^+$ uptake in cells expressing the individual charge-reversal mutants (Fig. 3A). The maximal exchange activity at pH_i 5.4 (V_{max}) was normalized with regard to the amount of surface NHE1, and these normalized values are summarized in Table 1. Whereas the Glu131 (E131R) mutation reduced the normalized activity to ~50%, most other mutations did not alter it to a great extent (Table 1). Interestingly, the pH_i dependence of the $^{22}Na^+$ uptake greatly shifted to the acidic side in the E131R and R327E mutants (Fig. 3B). It should be particularly noted that the steepness of the pH_i dependence curve was highly reduced in E131R, i.e. the Hill coefficient reached approximately 1.0; this result was in sharp contrast to those of all other NHE1 variants, which yielded a higher Hill coefficient of more than 1.0 (Table 1). Furthermore, the pH_i dependence slightly shifted to the alkaline side in D448R and R500E (Fig. 3B). Thus, we identified several charge-reversal mutations (E131R, R327E, D448R, and R500E) that affected the pH_i dependence of the Na^+/H^+ exchanger.

We further constructed some NHE1 mutants at Glu131 (E131Q, E131D and E131K) and measured the pH_i dependence of $^{22}Na^+$ uptake in cells expressing these mutant exchangers. These mutant proteins were well expressed in cells, although the surface expression levels appeared to be slightly lower than that of the wild-type NHE1 (data not shown). We found that charge-preserved mutation (E131D) had no effect on pH_i dependence, suggesting that mutation itself does not much influence the function of NHE1. In contrast, charge-reversal substitution of E131 with another positive residue, Lys, similar to Arg, resulted in a large acidic shift of pH_i dependence as well as a decrease in the normalized V_{max} (Table 1). Thus, the charge of E131 appears to be important for the normal function of NHE1. Furthermore, we found that charge neutralization (E131Q) also resulted in a slight decrease in p*K*a.

Various extrinsic factors are known to activate NHE1 and bring about long-lasting cytoplasmic alkalinization, particularly in the absence of bicarbonate [1–6]. As shown in Fig. 4, thrombin, the protein kinase C activator 4β-phorbol 12-myristate 13-acetate and hyperosmotic stress (200 mM sucrose) all induced a high level of cytoplasmic alkalinization in cells expressing wild-type NHE1, D448R, or R500E. In contrast, such alkalinization was completely absent in cells expressing E131R or R327E (Fig. 4), suggesting that

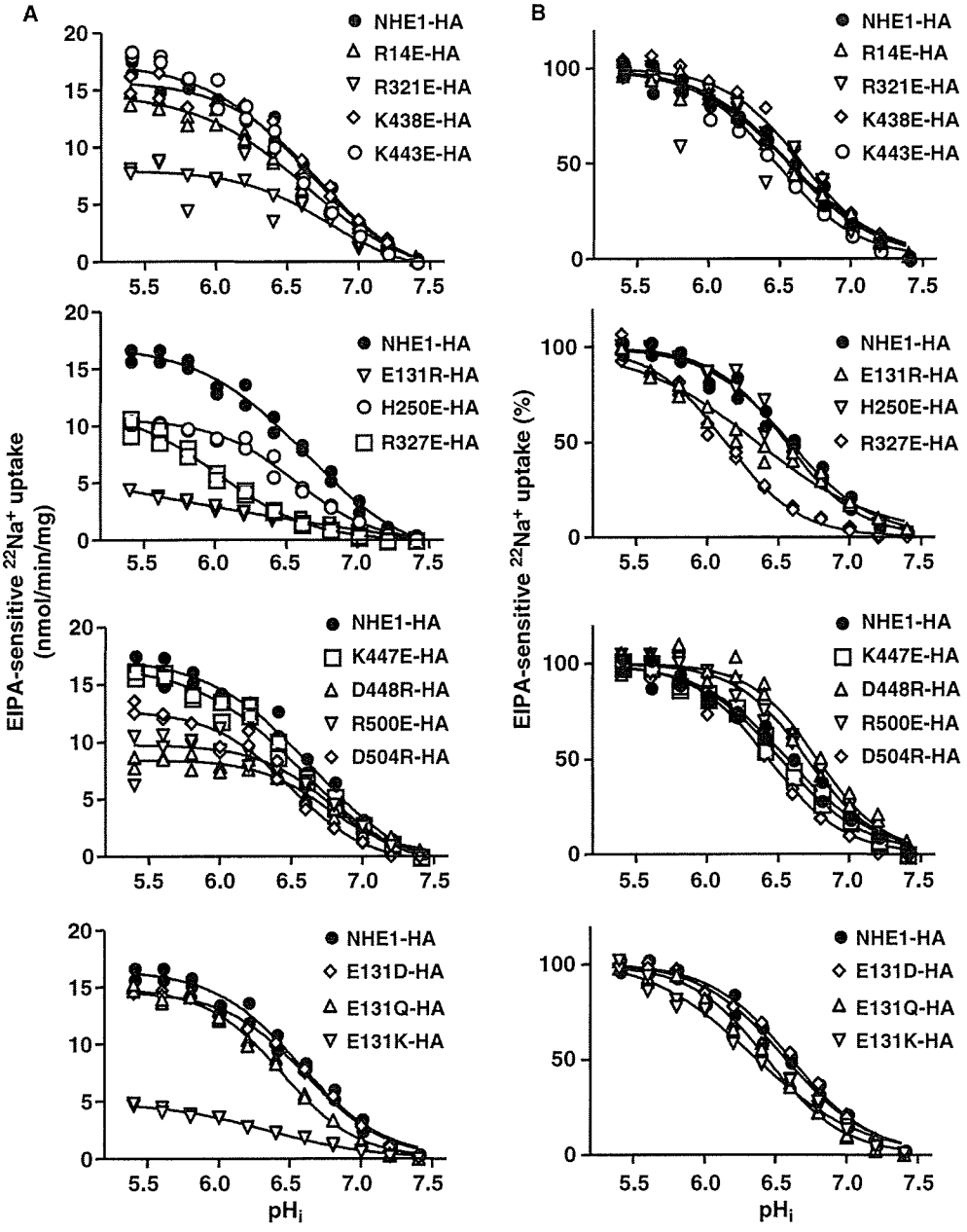

Fig. 3. The pH$_i$ dependence of EIPA-sensitive $^{22}Na^+$ uptake. (A) $^{22}Na^+$ uptake was measured in cells expressing the wild-type or mutant exchangers in the presence or absence of 0.1 mM EIPA after pH$_i$ clamping at various values with K^+/nigericin. The wild-type or mutant exchangers exhibited high maximal $^{22}Na^+$ uptake activities (4–20 nmol·mg^{-1}·min^{-1} at pH$_i$ 5.4). Data were fitted to the sigmoidal dose dependence equation as described in 'Experimental procedures'. (B) Data are normalized to the maximal uptake activity at pH$_i$ = 5.4.

these residues are important for the physiologic response of the exchanger. NHE1 is thought to be activated in response to external stimuli via alkaline shift of a 'pH set-point', i.e. pH$_i$ dependence [1]. The lack of alkalization in cells expressing these NHE1 mutants would be due to their low exchange activity in the neutral pH$_i$ range, resulting from the acidic shift of pH$_i$ dependence, even in the case that extracellular stimuli had slightly activated these mutants via an alkaline shift. In previous studies, we identified many mutations resulting in a large acidic shift of pH$_i$ dependence and in a lack of cytoplasmic alkalinization [15,19,23].

Table 1. Kinetic parameters for the pH_i dependence of $^{22}Na^+$ uptake. The pH_i dependence of EIPA-sensitive $^{22}Na^+$ uptake (Fig. 3) was fitted to a sigmoidal dose-dependent equation. The best fitted value with standard error is represented for p*K* and the Hill coefficient. The V_{max} value is the $^{22}Na^+$ uptake activity at pH_i 5.4 (means ± SD, $n = 3$). The relative amount of surface-expressed NHE1 was calculated from the amounts of total and streptavidin bead-absorbed proteins, and the V_{max} value was normalized (means ± SD, $n = 3$).

NHE1 variants (%)	p*K* for pH_i	Hill coefficient	V_{max} (nmol·mg^{-1}·min^{-1})	Normalized V_{max}
NHE1	6.57 ± 0.02	1.40 ± 0.08	16.19 ± 0.55	100.0
R14E	6.56 ± 0.02	1.40 ± 0.07	13.77 ± 1.04	103.7 ± 8.1
E131R	6.35 ± 0.03	1.00 ± 0.07	4.24 ± 0.32	55.0 ± 9.6
H250E	6.56 ± 0.02	1.68 ± 0.09	10.42 ± 0.12	85.5 ± 1.2
R321E	6.57 ± 0.05	1.30 ± 0.17	8.39 ± 0.70	89.7 ± 3.2
R327E	6.13 ± 0.02	1.68 ± 0.10	9.93 ± 0.72	151.6 ± 22.0
K438E	6.66 ± 0.02	1.60 ± 0.12	15.85 ± 0.96	100.8 ± 8.0
K443E	6.48 ± 0.02	1.51 ± 0.07	18.25 ± 0.20	118.4 ± 9.7
K447E	6.52 ± 0.01	1.48 ± 0.07	16.09 ± 0.30	111.1 ± 7.0
D448R	6.78 ± 0.02	1.84 ± 0.16	8.64 ± 0.07	146.0 ± 11.6
R500E	6.71 ± 0.02	1.73 ± 0.10	10.17 ± 0.50	100.1 ± 7.4
D504R	6.43 ± 0.02	1.65 ± 0.10	12.88 ± 0.62	82.7 ± 4.4
E131Q	6.44 ± 0.02	1.62 ± 0.10	14.66 ± 0.65	126.4 ± 8.1
E131D	6.61 ± 0.02	1.53 ± 0.08	14.63 ± 0.12	135.6 ± 16.4
E131K	6.34 ± 0.05	1.16 ± 0.10	4.68 ± 0.20	57.7 ± 2.9

As E131R exhibited an unusual pH_i profile, we were interested in the other kinetic properties of this NHE1 mutant. Figure 5A shows the dependence of $^{22}Na^+$ uptake on the external Na^+ concentration ($[Na^+]_o$). Interestingly, E131R was observed to have a higher affinity for Na^+ as compared to the wild-type NHE1 (K_m, 1.6 mM versus 6.0 mM; Table 2). Similarly, it also exhibited a higher affinity for Li^+. However, the extracellular pH dependence did not differ between wild-type NHE1 and E131R (Table 2). Furthermore, the NHE1 affinity for the inhibitor EIPA also increased slightly following this mutation (Fig. 5B and Table 2). These results suggest that Glu131 is important for transported cation binding as well as pH_i-sensitivity regulation.

Discussion

In this study, we analyzed the effect of charge-reversal mutations that were introduced in charged residues located in the intracellular loops of NHE1 on the function of this molecule. The surface expression levels and normalized exchange activity (V_{max}) of NHE1 were not drastically altered for molecules with 11 tested mutations, suggesting that these mutant exchangers exhibit normal protein folding, proper membrane targeting, and relatively high transport activity. However, we were unable to obtain the stable expression of E247R by using an activity-dependent selection procedure. Among the NHE isoforms, Glu247 located in TM6 or IL3 is highly conserved and may play a critical role in cation transport and/or membrane expression. We observed that the substitution of Glu131 with Arg shifted the pH_i dependence of the Na^+/H^+ exchange to the acidic side, whereas mutations at Asp448 and Arg500 induced a slight alkaline shift. In addition, we confirmed a previous result [20] that charge-reversal mutation of Arg327 brought about a large acidic shift. Thus, the present study provides reasonable evidence that the side chains of charged residues located in the intracellular loops of NHE1 may play an important role in pH_i regulation by this molecule.

Although NHE1 catalyzes electroneutral Na^+/H^+ counter-transport, it is also known to be a highly proton-dependent transporter [1]. Whereas NHE1 is activated with an increase in the cytosolic H^+ concentration, it is completely inactivated at $pH_i > \sim 7.4$ (pH set-point). There is substantial evidence that this fascinating function of NHE1 can be attributed to the existence of cytosolic H^+-modifier site(s) distinct from its cation transport site [1,9–11]. For example, we previously reported that $^{22}Na^+$ efflux from cells expressing NHE1 can be activated by mild cytosolic acidification only from pH 7.4 to 7.2, implying the existence of an H^+-regulatory site(s) that is required for H^+-induced activation of NHE1 [11]. Furthermore, the steep activation curve for $^{22}Na^+$ efflux suggested that protonation of multiple amino acid side chains may be involved in the regulation of pH_i sensing by NHE1 [11]. The involvement of multiple protons was also suggested in a recent kinetic study on